

BEAM CHARACTERISTICS OF MECHANICALLY TUNABLE MAGNETRON INJECTION GUNS

Yi Sheng Yeh¹, Tsun-Hsu Chang², and Chao-Ta Fan²

*¹Department of Electrical Engineering
Southern Taiwan University of Technology
Tainan, Taiwan*

*²Department of Physics
National Tsing Hua University
Hsinchu, Taiwan*

Received May 1, 2001

ABSTRACT

Gyrotron has received extensive attention owing to its high-power capability, particularly when the wavelength shrinks below the millimeter-wave range. The electron beam of a gyrotron is typically generated by a magnetron injection gun (MIG), and a mechanically tunable MIG is employed to enhance the beam quality. However, a slight adjustment in the position of the center electrode of the mechanically tunable MIG can cause significant modification of the electric-field profile. Consequently, the cathode current of the mechanically tunable MIG is not only dependent on the cathode temperature, but also the relative position of center electrode. To accurately determine the beam characteristics of the mechanically tunable MIG, an improved computer program is employed to simulate electron trajectories. Simulation and measurement results indicate that although the magnetic field and compression ratio do not influence the beam current of the mechanically tunable MIG, but the beam current of the MIG depends on the cathode temperature and relative position of the center electrode. Finally, an improved mechanically tunable MIG design is developed to enhance an beam quality while minimizing beam current variation.

Key words: Magnetron injection gun, mechanically tunable magnetron injection gun, gyrotron, gyro-TWT

I. INTRODUCTION

Various gyrodevices based on fast-wave interaction structures, such as gyrotrons, the peniotrons, and the cyclotron autoresonance maser, are currently receiving attention owing to their capacity for high-power millimeter-wave generation [1]. The electron beam of such devices is typically generated by a magnetron injection gun [2, 3]. In a MIG, electrons originate from a ring-shaped thermionic emitter mounted on the cathode. An electric field extends between the cathode and the anode, and a static magnetic field is applied to bend, as well as focus the electrons. As soon as leaving the cathode, the electrons experience a crossed electric and magnetic field, thereby obtaining the spiral motion. The electrons thus form an annual beam with electrons executing small cyclotron orbits, as required for the cyclotron resonance interaction.

The electric-field profile between the cathode and anode is most sensitive to the configuration of the cathode surface. A single anode MIG (Figs. 1 and 2) capable of mechanical tunability was developed by National Tsing Hua University (NTHU) [4, 5]. Rather than the conventional approach of assembling the cathode in one solid piece, the tip of the cathode is designed as a mechanically detached piece referred to as the center electrode fitted through the emitter ring. Therefore, a tuning mechanism is provided by the axial movement of the center electrode with respect to the

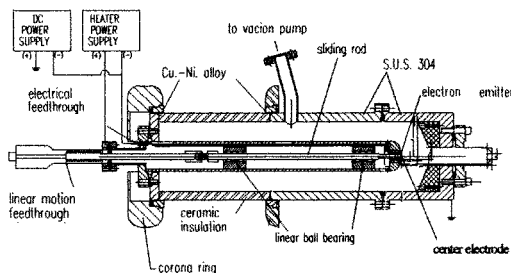


Fig. 1. Side view of the essential portion of the mechanically tunable single-anode MIG under study.

rest of the cathode assembly. Since the accelerating electric-field reaches its maximum around the tip of the cathode, a slight adjustment in the position of the center electrode can significantly modify the electric-field profile and, hence the beam formation processes. In contrast to the intermediate anode tuning, which shapes the electric field from outside the annular electron beam, the center electrode tuning shapes the electric field from inside the beam annulus. Therefore, the center electrode tuning method can be applied to double-anode MIGs as a complementary tuning mechanism.

Previous gyro-TWT [4, 5] assumes that the operating point of the mechanically tunable MIG is in the temperature limited region. The cathode current is thus dominated by the cathode temperature. However, a slight adjustment in position of the center electrode of the mechanically tunable MIG can significantly modify the electric-field profile. The beam current of the mechanically tunable MIG is thus not only dependent on the cathode temperature, but also the relative position of center electrode. The beam characteristic of the mechanically tunable MIG is similar to the MIG operating between the space-charge and temperature limited regions.

Baird and Lawson [2] suggested that the operating point of a MIG is estimated by the ratio of the temperature limited cathode current density J_{TL} to the Langmuir space-charge limited current density J_{SC} in the trade-off equations. The design in which $J_{TL}/J_{SC} < 15\%$ is generally free of space-

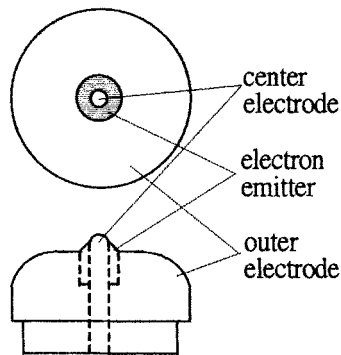


Fig. 2. Front view and side view of the cathode assembly.

charge problems, but merely estimates the value of J_{TL}/J_{SC} . Longo [6] found that the operating point of the thermionic emitter is generally the transition from the temperature limited to the space-charge limited region. Longo has employed an empirical law to study the cathode current density as a combination of both temperature limited and space-charge limited current density.

To accurately determine the beam characteristics of the mechanically tunable MIG, an improved computer program [7] is employed to simulate electron trajectories. The program permits operating regions between temperature limited and space-charge limited emission, and the initial input formation of the program is described using the input formation of the EGUN code [8]. The simulated cathode current density calculated from Langmuir's and Richardson's laws [9, 10] is dependent on the cathode temperature and the electric field of the cathode surface. The improved computer program [7] thus seems to be appropriate for the mechanically tunable MIG.

The rest of this paper is organized as follows. Section II describes the computer model of the program. Section III then presents the beam characteristics of the mechanically tunable MIG with different magnetic fields, compression ratios, cathode temperatures, and the relative positions of the center electrode. Furthermore, the measured results of the beam current obtained from the laboratory electron gun are presented and compared with the simulation results. Subsequently, Section IV develops an improved mechanically tunable MIG design is developed for enhancing the beam quality while minimizing beam current variation. Conclusions are finally made in Section V.

II. COMPUTER MODEL

The computer program is specifically designed for calculating electron trajectories in electrostatic and magnetostatic fields. In the steady state, the potential given by the Poisson equation can be expressed as

$$\nabla^2\Phi = -\frac{\rho}{\epsilon_0}, \quad (1)$$

where Φ is the electrostatic potential, ρ is the space-charge density, and

ε_0 is the permittivity in the vacuum. The Poisson equation is solved by the finite different method. Meanwhile, the semi-iterative Chebyshev method is used to shorten the calculation time [8].

The electron trajectories are determined by the relativistic force equation using the fourth-order Runge-Kutta method [8]

$$m \frac{d}{dt}(\gamma \mathbf{v}) = e \nabla \Phi - e \mathbf{v} \times \mathbf{B}, \quad (2)$$

where m is electron mass, γ is a factor of relativity, \mathbf{v} is the velocity of electron, e is the magnitude of electron charge, and \mathbf{B} is the total magnetic field including external and self-consistent magnetic fields.

The operating point of the cathode emitter may be in the region between the temperature limited and space-charge limited emission, so the cathode current density J_c from Longo's empirical formula can be expressed as a combination of the temperature limited current density J_{TL} and space-charge limited current density J_{sc} [9, 10]

$$J_c = \frac{J_{sc} + J_{TL}}{J_{sc} J_{TL}}. \quad (3)$$

The J_{sc} and J_{TL} calculated from Langmuir's and Richardson's laws [9, 10] are expressed as

$$J_{sc} = k \frac{\Phi^{3/2}}{d^2}, \quad (4)$$

$$J_{TL} = 1.2 \times 10^4 T^2 \exp\left(\frac{-11600W}{T}\right) \exp\left(0.44 \frac{\sqrt{E_n}}{T}\right), \quad (5)$$

where $k = (4/9)\varepsilon_0 \sqrt{(2e/m)} = 2.335 \times 10^{-6}$ (MKS), d is the normal distance from cathode (cm), W is the cathode work function (eV), T is the temperature of cathode ($^{\circ}$ K), and E_n is the component of the electric field normal to the cathode (V/m).

III. NUMERICAL SIMULATION AND EXPERIMENTAL VERIFICATION

A mechanically tunable MIG [4, 5] was developed at NTHU for a

Ka-band, TE_{11} mode gyro-TWT. The specifications of the gyro-TWT were $V_b = 93.6$ kV, $I_b = 3$ A, $B_0 = 12.5$ kG, $\alpha = 0.9$, and $\Delta v_z / v_z < 4\%$. Figure 3 displays a computer drawn cross-section of the final MIG configuration along with electron trajectories and a superimposed plot of the axial magnetic field profile.

Figure 4 displays the variation of the beam current with the axial magnetic field in the mechanically tunable MIG. The velocity ratio decreased with increasing the axial magnetic field, and the simulated beam currents do not appear to be dependent on the axial magnetic field. The measurement results are consistent with the simulation results.

Figure 5 displays the beam characteristics as functions of the compression ratio. Velocity ratio increased with the compression ratio increased, while the beam current remained constant. The simulation results correlate with the measurement results.

Figure 6 displays the simulated and measured beam currents of the mechanically tunable MIG at the different beam voltages. As Fig. 6a illustrates, the space-charge limited current increased with the anode voltages. Meanwhile Fig. 6b shows the measurement results of the MIG. The simulation results are consistent with the measured results.

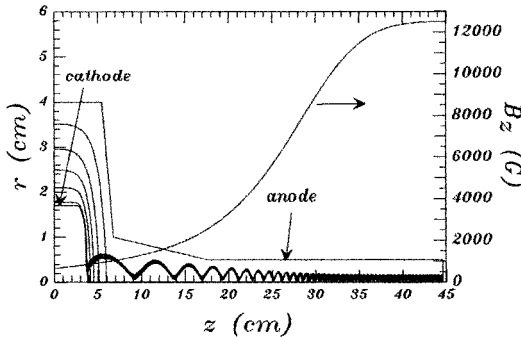


Fig. 3. Schematic of a MIG for a Ka-band, TE_{11} mode gyro-TWT and calculated electron trajectories. Also shown are the equal-potential lines and the magnetic field profile. Radial and horizontal axes are scaled in unit of 0.025 cm.

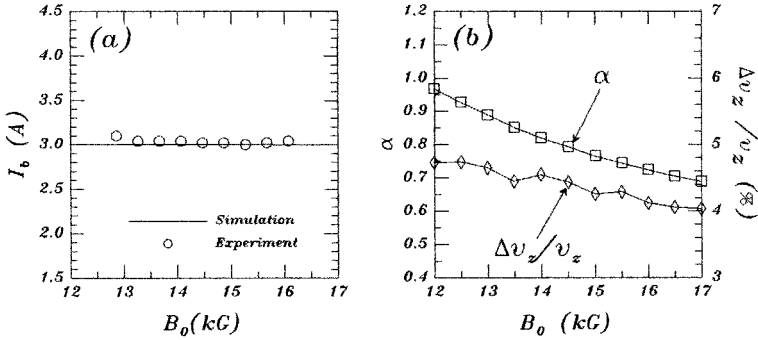


Fig. 4. (a) displays simulated and measured beam currents as functions of the axial magnetic field. (b) shows simulated velocity ratio α and axial velocity spread $\Delta v_z / v_z$ as functions of the axial magnetic field. The schematic of the MIG is shown in Fig. 2.

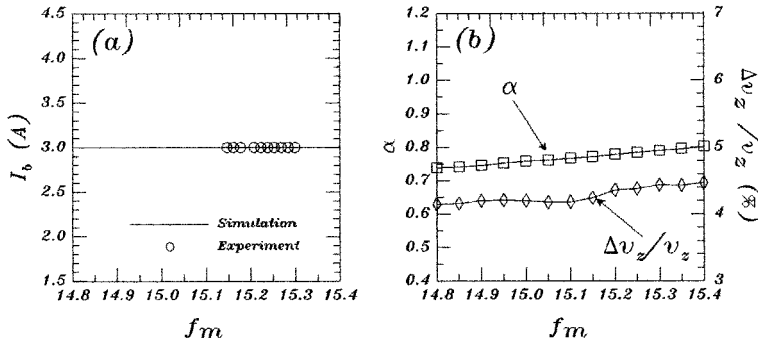


Fig. 5. (a) displays simulated and measured beam currents as functions of the compression ratio. (b) shows simulated velocity ratio α and axial velocity spread $\Delta v_z / v_z$ as functions of the compression ratio. The schematic of the MIG is shown in Fig. 2.

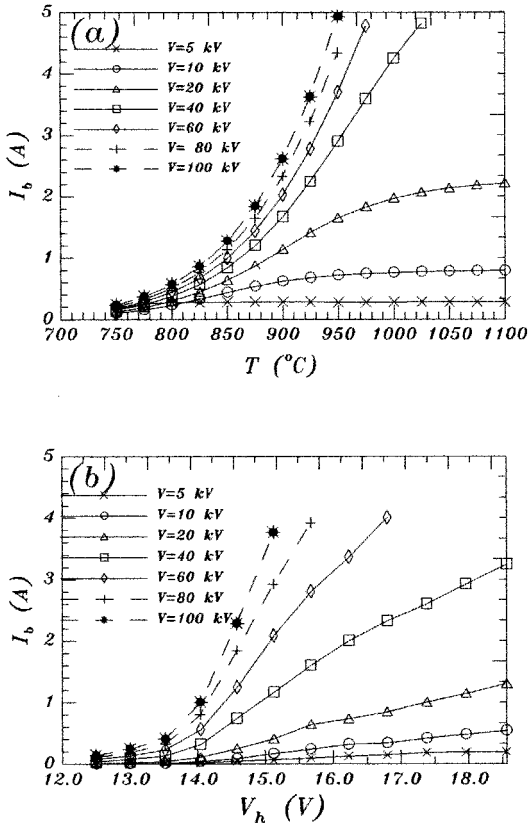


Fig. 6. (a) displays the simulated beam current at seven values of anode voltage as functions of the cathode temperature. The work function of the cathode is fixed to be 1.60 eV. (b) shows the measured beam current at seven values of anode voltage as functions of the heater voltage. The schematic of the MIG is shown in Fig. 2.

Figure 7 displays the beam characteristics as functions of the relative positions of the center electrode. Figure 7a indicates that the simulated and measured beam currents decrease as the relative positions of the center electrode increase. Meanwhile, Fig. 8 shows that the electric-potential profile of the cathode surface varies with the relative positions of the center electrode. Consequently, the variation of the beam current of the mechanically tunable MIG is influenced by the variation of the electric field of the cathode surface as the center electrode moves. However, the variation of the beam current is larger for the measured results than for the simulated results as the center electrode moves. The discrepancy between the measured and simulated results would be attributed to the current density can not be completely described in Longo's empirical formula (Eq. 3). Longo's empirical formula calculates the space-charge current density from Langmuir's law (Eq. 4), a formula that is appropriate for a parallel plane diode [9]. If the relative position variation of the center electrode is obvious, the parallel plane diode model appears inappropriate for simulating the electric field between the cathode and anode of the mechanically tunable MIG. Therefore, Langmuir's law appears somewhat inappropriate for calculating the beam current of the

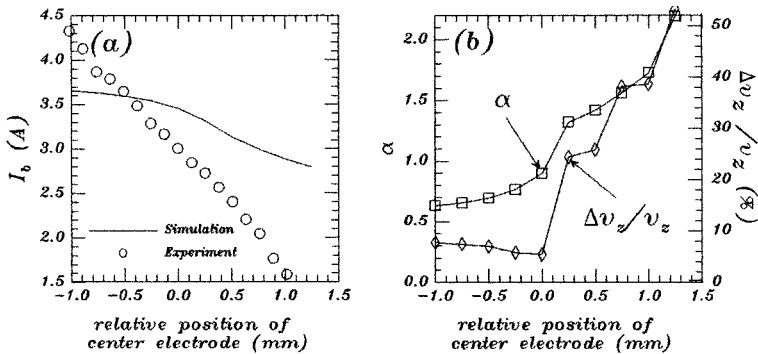


Fig. 7. (a) displays simulated and measured beam currents as functions of the relative position of the center electrode. (b) shows simulated velocity ratio α and axial velocity spread $\Delta v_z / v_z$ as functions of the relative position of the center electrode. The schematic of the MIG is shown in Fig. 2.

mechanically tunable MIG when the relative position variation of the center electrode is obvious.

IV. IMPROVED MECHANICALLY TUNABLE MIG DESIGNS

To enhance the beam quality of MIGs, the mechanically tunable MIGs are employed for tuning the beam quality of the MIGs, but the beam current

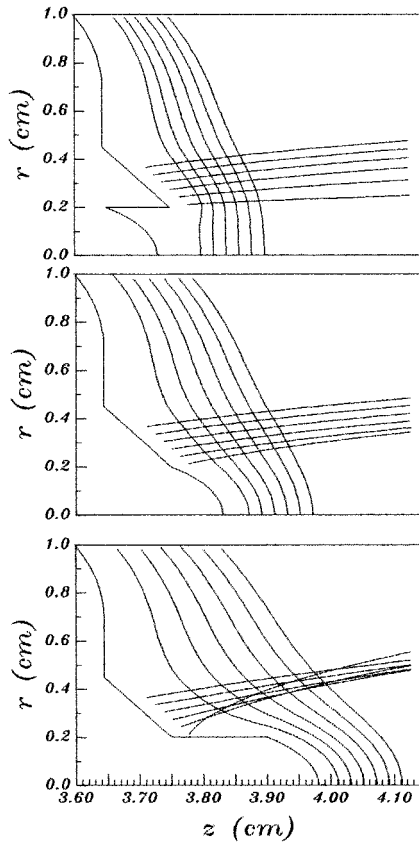


Fig. 8. Simulated equal-potential lines and electron trajectories near the cathode tip as the center electrode position is varied.

is influenced as the center electrode of the mechanically tunable MIG moves. The main goal of this section is to find mechanically tunable MIG designs which can enhance beam quality while minimizing beam current variation.

The beam current of the pervious mechanically tunable MIG design (Fig 2) is operating in 3A. The variation of the beam current is apparently influenced by the movement of the center electrode, as shown in Fig. 7. Clearly, the beam characteristics are sensitive to the relative position of the center electrode. To degrade the variation of the beam current, an improved mechanically tunable MIG design is developed as shown in Fig. 9. The center electrode divides into two separate parts, movable and fixed center electrodes. Meanwhile, the beam characteristics of the MIG as functions of the relative position of the center electrode are shown in Fig. 10. The variation of beam current and quality is less than for the pervious MIG (Fig. 2). Consequently, the MIG (Fig. 9) appears insensitive to the relative position of the center electrode

On the other hand, mechanically tunable MIG designs are not necessary to be modified to degrade the variation of the beam current at all. For instance, Fig. 11 shows a schematic of a mechanically tunable MIG which was developed for Ka-band TE_{01} gyro-TWT [7]. The specifications of gyro-TWT are $V_b=90$ kV, $I_b=20$ A, $B_0=12.8$ kG, $\alpha=0.9$, $\Delta v_z/v_z < 5\%$, and $r_g=0.28$ cm. Figure 12 displays the beam characteristics as functions of the relative position of the center electrode. The simulation results indicate that the variation ratio of the beam current $\Delta I_b / I_b$, velocity ratio α , and velocity spread $\Delta v_z/v_z$ is less for this MIG (Fig. 11) than for the previous MIG (Fig. 3). The difference may be attributed to the cathode current not being determined only by the electric filed of the cathode surface. Consequently, the beam current is not proportional to the electric filed of the cathode surface. Previous research [7] reported that the simulated temperature limited and space-charge limited currents of the MIG are 21.1 A and 395 A, respectively. From Longo's empirical formula (Eq. 3), the beam current is dominated by the cathode temperature. The variation ratio of beam current $\Delta I_b / I_b$ is less obvious for this MIG than for the previous MIG. Therefore, the mechanically tunable MIG design does not need to be modified to enhance the beam quality while minimizing beam current variation.

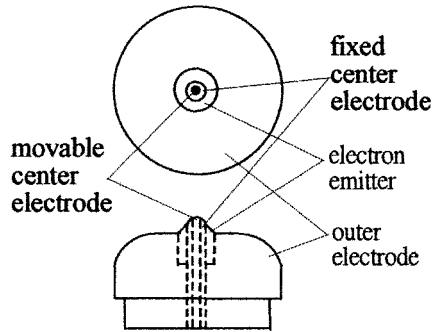


Fig. 9. Front view and side view of the cathode assembly of the improved mechanically tunable MIG

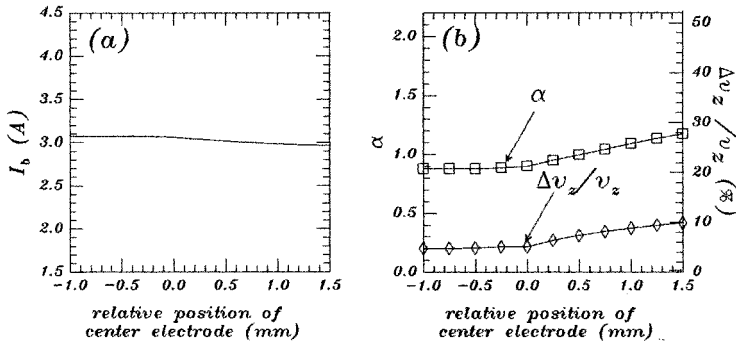


Fig. 10. (a) displays simulated and measured beam currents as functions of the relative position of the center electrode. (b) shows simulated velocity ratio α and axial velocity spread $\Delta v_z/v_z$ as functions of the relative position of the center electrode. The schematic of the MIG is shown in Fig. 9.

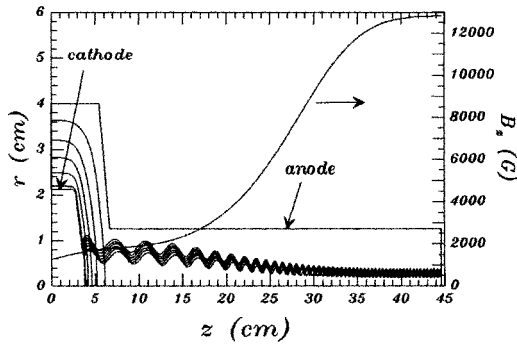


Fig. 11. Schematic of a MIG for a Ka-band, TE_{01} mode gyro-TWT and calculated electron trajectories. Also shown are the equal-potential lines and the magnetic field profile. Radial and horizontal axes are scaled in unit of 0.025 cm.

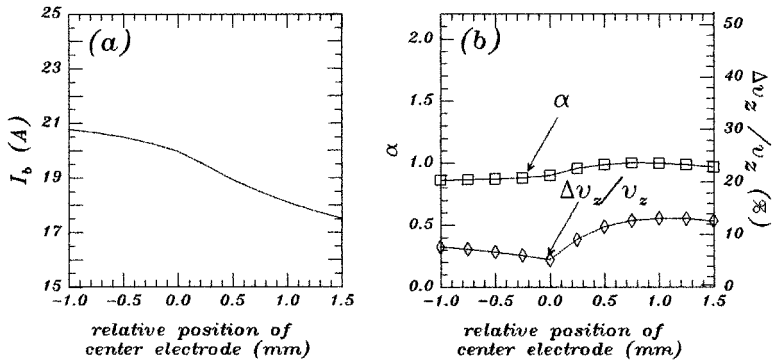


Fig. 12. (a) displays simulated beam currents as functions of the relative position of the center electrode. (b) shows simulated velocity ratio α and axial velocity spread $\Delta v_z/v_z$ as functions of the relative position of the center electrode. The schematic of the MIG is shown in Fig. 11.

V. CONCLUSIONS

The beam characteristics of a mechanically tunable MIG were studied by using an improved computer program. The beam current of the mechanically tunable MIG is not influenced by the magnetic field and compression ratio, but is dependent on the cathode temperature and the relative position of the center electrode. Finally, an improved mechanically tunable MIG design is developed to enhance the beam quality while minimizing beam current variation.

We recommend that an modified Langmuir's law which is not restricted to a parallel diode would be developed for calculating the space-charge limited current density. The model might be useful for simulating the beam characteristics of the mechanically tunable MIG correctly.

ACKNOWLEDGMENTS

The authors would like to thank Prof. K.R. Chu and T.T. Yang for their valuable assistance and cooperation. This work was supported by the National Science Council of the Republic of China (NSC-89-2213-E-218-038).

REFERENCES

- [1] J.L. Seftor, A.T. Drobot, and K.R. Chu, "An investigation of a magnetron injection gun suitable for use in cyclotron resonance maser," *IEEE Trans. Electron Devices*, vol. ED-26, no. 10, pp. 1609-1616, 1979.
- [2] J.M. Baird and W. Lawson, "Magnetron injection gun (MIG) design for gyrotron applications," *Int. J. Electron.*, vol. 61, no. 6, pp. 953-967, 1986.
- [3] K.R. Chu, L.R. Barnett, W.K. Lau, L.H. Chang, and H.Y. Chen, "A wide-band millimeter-wave gyrotron traveling wave amplifier experiment," *IEEE Trans. Electron Devices*, vol. 37, no. 6, pp.

- 1557-1560, 1990.
- [4] K.R. Chu, L.R. Barnett, H.Y. Chen., S.H. Chen, Ch. Wang, Y.S. Yeh, Y.C. Tsai, T.T. Yang, and T.Y. Dawn, "Stabilization of absolute instabilities in the gyrotron traveling wave amplifier", *Phys. Rev. Lett.*, vol. 74, no. 7, pp. 1103-1106, 1995.
 - [5] Ch Wang, Y.S. Yeh, T.T. Yang, H.Y. Chen, S.H. Chen, Y.C. Tsai, L.R. Barnett, and K.R. Chu, "A mechanically tunable magnetron injection gun," *Rev. Sci. Instruments*, vol. 68, no. 8, pp. 3031-3035, 1997.
 - [6] R.T. Longo, "A study of thermionic emitters in the regime of partial operation," *Int. Electron Devices Mtg.*, p467-470, 1980.
 - [7] Y.S. Yeh, M.H. Tsao, H.Y. Chen, and T.H. Chang, "Improved computer program for magnetron injection gun design", *Int. J. Infrared and Millimeter Waves*, vol. 21, no.9, pp.1397-1415, 2000.
 - [8] W.B. Herrmannsfeldt, *Electron Trajectory Program*, Stanford Linear Accelerator Center Report SLAC-226, 1979.
 - [9] R.B. True, *Space-charge-limited beam forming systems analysed by the method of self-consistent fields with solution of Poisson's equation on a deformable relation mesh*, Ph.D. thesies, University of Connecticut, 1972.
 - [10] M. Caplan and C. Thorington, "Improved computer modelling of magnetron injection guns for gyrotrons," *Int. J. Electron.*, vol. 51, no. 4, pp. 415-426, 1981.